Published in final edited form as:
ACS Chem Biol. 2011 August 19; 6(8): 775–780. doi:10.1021/cb200100f.

H-bond network around retinal regulates the evolution of ultraviolet and violet vision

Ahmet Altun[†,‡,§], **Keiji Morokuma**[†,¶,*], and **Shozo Yokoyama**[‡,*]

[†] Cherry L. Emerson Center for Scientific Computation and Department of Chemistry, Emory University, Atlanta, GA 30322, USA

[‡] Department of Biology, Rollins Research Center, Emory University, 1510 Clifton Road, Atlanta, GA 30322, USA

[§] Department of Physics, Fatih University, 34900 B. Cekmece, Istanbul, Turkey

[¶] Fukui Institute for Fundamental Chemistry, Kyoto University, 34–4 Takano Nishihirakicho, Sakyo, Kyoto 606–8103, Japan

Abstract

Ancestors of vertebrates used ultraviolet vision. Some descendants preserved ultraviolet vision while some others replaced it with violet vision, and then, some of avian lineages reinvented ultraviolet vision. Ultraviolet (absorption at ~360 nm) and violet (410–440 nm) sensitivities of visual pigments are known to be affected by around 20 amino acid substitutions. The present quantum mechanical/molecular mechanical calculations show that these substitutions modify a H-bond network formed by two waters and sites 86, 90, 113, 114, 118 and 295, which determines the protonation state of Schiff base-linked 11-*cis*-retinal. A pigment is ultraviolet-sensitive when it is more stable with an unprotonated retinal (SBR) form than with its protonated analog (PSBR), and is violet-sensitive when the PSBR form is more stable. These results establish for the first time the chemical basis of ultraviolet and violet vision in vertebrates.

The chromophore 11-*cis*-retinal in solution has a λ_{max} of 440 nm in its protonated form (1) and 365 nm in the unprotonated form (2). However, by interacting with various short wavelength-sensitive type 1 (SWS1) opsins, the retinals achieve a diverse range of λ_{max}s between 360 and 440 nm (3). Mutagenesis experiments using E113Q suggested that the chromophores of ultraviolet and violet pigments are SBR and PSBR, respectively (4–7). We have already verified (8) these experimental suggestions for the mouse ultraviolet and human violet SWS1 pigments by using a hybrid quantum mechanical/molecular mechanical (QM/MM) method in Our own *N*-layer Integrated molecular Orbital and Molecular Mechanics (ONIOM) scheme (9), which was developed for calculating structural, energetic and spectroscopic properties of large molecules. ONIOM and analogues QM/MM methods have proven useful in investigating spectral tuning mechanisms of both rod and cone pigments (10–15).

Corresponding authors: Dr. Shozo Yokoyama: Department of Biology, Rollins Research Center, Emory University, 1510 Clifton Road, Atlanta, GA 30322 [Tel: (404) 727-5379; FAX: (404)727-2880; syokoya@emory.edu]. Dr. Keiji Morokuma: Cherry L. Emerson Center for Scientific Computation and Department of Chemistry, Emory University, Atlanta, GA 30322, USA [Tel: (404) 727-2180; FAX: (404)727-7412; morokuma@emory.edu].

Internet at http://pubs.acs.org.

Author contributions: S.Y. conceived and designed research; A.A. and K.M. designed the QM/MM analyses; A.A. performed the calculations; S.Y., A.A., and K.M. wrote the paper.

Supporting Information Available: This material is available free of charge via

Because of strong amino acid interactions (7, 16, 17), the analyses based on contemporary pigments may misidentify amino acid changes that cause λ_{max}-shifts and thus may result in erroneous spectral tuning mechanisms (3, 18). For example, it is known that the λ_{max}s of *mouse (P359)* and *human (P414)* can be interchanged by seven amino acid changes; however, when these amino acid changes are introduced into *mouse (P359)* individually, none of the single mutations shifts the λ_{max} (16). Amino acid interactions cause serious problems not only in identifying functionally important amino acid changes correctly but also for deriving the correct molecular mechanism of spectral tuning. Fortunately, these problems can be alleviated by genetically engineering "ancestral" pigments and introducing amino acid changes into them rather than into contemporary pigments (3, 18). Even then, the experimental results do not reveal how such amino acid changes actually cause the λ_{max}-shift. It is QM/MM calculations performed on ancestral SWS1 pigments that can provide such critical information on the structure-function relationships.

So far, the evolutionary changes of SWS1 pigments have been experimentally studied along four lineages (Figure 1, panel a): 1) *pigment a* to *scabbard (P423)* of scabbardfish (19), 2) *pigment d* to *frog (P425)* of African clawed frog (17), 3) *pigment f* to *pigment g* (4), and 4) *pigment f* to the ultraviolet pigments of budgerigar, canary, and zebra finch (4). The evolutionary changes from *pigment h* to *human (P414)* (16), *bovine (P438)* (7), and *elephant (P419)* (20) have also been inferred by manipulating contemporary pigments. All of these mutagenesis analyses suggest that the evolutionary switches between ultraviolet and violet pigments have been caused by 1–7 amino acid changes (21) at a total of 12 sites in transmembrane helices (TM) I–III (Figure 1, panel b).

Here we have investigated the chemical mechanism that is responsible for the evolutionary switch between ultraviolet and violet vision by performing ONIOM (QM/MM) calculations on the modeled ultraviolet-sensitive *pigment a*, *pigment d*, *pigment f*, *pigment h* (Figure 1, panel a), and their mutants. Therefore, this theoretical study covers all vertebrate evolution pathways currently known.

In order to assess if the Schiff-base (SB) nitrogen linked to 11-*cis*-retinal is protonated or deprotonated, we evaluated the ground-state energy of each pigment with SBR subtracted from that with PSBR (ΔE). The results (Table 1) show that the ultraviolet pigments (λ_{max} = 359–366 nm) have ΔEs = *E(SBR) – E(PSBR)* of 2.5–8.3 kcal·mol^{-1} and thus are more stable with SBR than with PSBR, whereas the violet pigments (λ_{max} = 411–421 nm) have the opposite relationship (ΔEs = −5.6 – −2.4 kcal·mol^{-1}). We also find that *pigment f′* (*pigment f* with four mutations F49V/F86S/L116V/S118A) with an intermediate λ_{max} of 393 nm has a ΔE of −0.3 kcal·mol^{-1}.

To demonstrate the effects of the three distinct sets of ΔEs on the absorption spectra of SWS1 pigments, we show *in vitro* spectra of three representative SWS1 pigments with various wavelengths (Supplementary Figure 1). *Pigment a* (ΔE = 6.2 kcal·mol^{-1}) and *human (P414)*, which is equivalent to *pigment h* with the seven mutations (ΔE = −3.1 kcal·mol^{-1}), have absorption spectra with single λ_{max}s of 360 and 414 nm, respectively. However, *pigment f′* generates a major peak at 393 nm and a shoulder at 410 nm as a result of the overlapped signals from its SBR and PSBR analogs that are roughly equally stable, or have similar proportions (Supplementary Figure 2b). This explains the origin of minor peaks found previously in some SWS1 pigments (4, 7, 16, 17).

In general, accurate evaluation of the vertical absorption wavelengths (λs) with presently available QM methods is a very challenging problem although the evaluation of spectral shifts is relatively easy (22). Consistent with previous findings, λs of pigments with SBR (410–425 nm), PSBR (475–482 nm), and roughly equal proportions of SBR and PSBR (443

nm) evaluated by the presently applied excited-state calculation method (TD-B3LYP) are consistently 50–60 nm higher than the corresponding experimental λ_{max}s of ~360, 411–424, and 393 nm, respectively (19). However, the deviation of the λ of any pigment from that of *pigment a* (Δλ) and the corresponding experimental result ($\Delta\lambda_{max}$) are very close to each other, indicating that stability order of PSBR and SBR analogs controls λ_{max}s of the SWS1 pigments (Table 1).

To search for the key structural changes that determine the relative stabilities of SBR and PSBR in various SWS1 pigments, we first compared the molecular structures of ancestral ultraviolet-sensitive *pigments a – f* and *h* along with those of three distantly related mutants; 1) *pigment f′* (equivalent to *pigment g*), 2) *pigment h* with F46T/F49L/T52F/F86L/T93P/A114G/S118T (equivalent to *human (P414)*), and 3) *pigment d* with F86M/V91I/T93P/V109A/E113D/L116V/S118T (equivalent to *frog (P425)*). The results show that *pigments a – f* and *h* have a H-bond between backbone O atom of A114 and side chain OH moiety of S118, and their chromophore-counterion H-bond distances (d_1s) between site 113 and SB nitrogen are 1.99 Å (e. g. Figure 2, panel a). In their mutant pigments, cleavage of the H-bond between sites 114 and 118 (or reduction of its strength) decreases the d_1s. For example, in *pigment f′*, Ala118 side chain moves significantly away from Ala114 and d_1 reduces to 1.79 Å (Figure 2, panel b). In the *pigment h* mutant, Thr118 moves away from Gly114 and decreases d_1 to ~1.80 Å (Figure 2, panel c); similar structural changes occur in the *pigment d* mutant as well.

To evaluate the effects of these structural changes on the relative stabilities of SBR and PSBR in SWS1 pigments, we calculated two quantities: 1) the difference between Δ*E*s of a particular pigment and its ancestral pigment (δ*E*) and 2) individual contributions to δ*E*s obtained by turning off the charges of some specific amino acids. The latter quantity appears to be a function of the modified H-bond distances $d_1 – d_3$ (Figure 2, panel d): the d_1 distance between Schiff-base nitrogen and Glu113 referred to as $\delta E_{113+114+118}$ (d_1), the d_2 distance between site 90 and Glu113 ($\delta E_{90+W1}(d_2)$) and the d_3 distance between site 86 and W2 ($\delta E_{86+W2}(d_3)$). The results show that the δ*E* generated during the evolution of *pigment f′* from *pigment f* is -4.1 kcal·mol^{-1}. This is fully explained by $\delta E_{113+114+118}$ (d_1) (Table 2). Similarly, the δ*E*s between *pigment d* and *frog (P425)* and between *pigment h* and *human (P414)* are ~ -11 kcal·mol^{-1}, which are also explained fully by the corresponding $\delta E_{113+114+118}$ (d_1) (Table 2).

The λ_{max}s of *elephant (P419)* and *bovine (P438)* seem to have evolved from *pigment h* mainly by F86S/L116V and F86Y, respectively. In these transitions, no amino acid change at site 118 is directly involved, but the δ*E*s of ~ -11 kcal·mol^{-1} generated can be explained mostly by $\delta E_{113+114+118}$ (d_1) (Table 2). In fact, $\delta E_{113+114+118}$ (d_1) either switches the SBR and PSBR in SWS1 pigments directly or making the changes more susceptible to the changes in d_2 and d_3. The latter case can be seen in the two consecutive evolutionary steps from *pigment f* to *pigment f′* and from *pigment f′* to *pigment f′* with S86C/S90C (4), where the total δ*E* of -0.7 kcal·mol^{-1} is explained by combining all $\delta E_{113+114+118}$ (d_1), δE_{86+W2} (d_3), and δE_{90+W1} (d_2) (Table 2). However, if only the second evolutionary step is considered, its δ*E* of 3.4 kcal·mol^{-1} is explained only by δE_{86+W2} (d_3) and δE_{90+W1} (d_2); essentially the same arguments hold between *pigment f′* and its single mutants. These results show that the change in d_1 is required before the PSBR of *pigment f′* eventually switches to SBR.

With the exception of the *pigment f′* mutants, the d_1 distance is shorter with PSBR than with SBR in violet-sensitive pigments while the reverse relation holds in ultraviolet-sensitive pigments (Supplementary Table 1). Therefore, violet-sensitive pigments are more stable with PSBR, whereas ultraviolet-sensitive pigments are more stable with SBR. In *pigment f′*,

the mutations do not significantly affect the d_1 distance. However, when S90C is introduced singly or with S86C into *pigment f′*, the d_2 distance increases; the increase is more pronounced with PSBR. Hence, SBR analogs of S90C and S86C/S90C mutants of *pigment f′* are more stable than the PSBR analogs. S86C mutation does not affect the d_2 distance much, but it increases the d_3 distance significantly. This increase is again more pronounced with PSBR, and thus the SBR form is more stable.

The violet-sensitive *scabbard (P423)* evolved from *pigment b* by the deletion of Phe86, but the same deletion in *pigment a* increases the λ_{max} only to 380 nm (19). *Pigment a* with Phe86-deletion has a δE of −0.4 kcal·mol^{-1}, whereas *pigment b* with Phe86-deletion has a δE of −9.4 kcal·mol^{-1} (Table 2). Hence, despite having the same ultraviolet-sensitivities, only *pigment b* responds to the deletion of Phe86 and increases its λ_{max} by ~60 nm. During the evolution from the *pigment a* to *pigment b*, δE is −3.0 kcal·mol^{-1} (19). However, δE difference between their Phe86-deletion analogs is −9.0 kcal·mol^{-1}, which has largest contribution from the change in d_1, and then, in d_2 and d_3. (Table 2). Hence, ultraviolet-sensitive *pigment a* and *pigment b* are structurally very different, especially around site 118 (19).

Experimental analyses of contemporary and engineered ancestral pigments have shown that ultraviolet- and violet-sensitivities of SWS1 pigments have been changed by various sets of amino acid changes on many occasions. To elucidate the molecular basis of spectral tuning in the SWS1 pigments, we analyzed all currently known amino acid changes that have generated not only ultraviolet and violet vision but also transitional steps in terms of QM/MM calculations. Our QM/MM analyses clearly show for the first time that the hydrogen-bond network near the retinal modified by these amino acid changes actually controls the stability order of SBR and PSBR analogs of SWS1 pigments and their λ_{max}s. The change in d_1 alone is enough for the evolutionary switch between UV and violet vision in many occasions. However, sometimes the changes in d_2 and d_3 must be associated with it. This conclusion is based on the amino acid changes in TM I–III. However, chimeric pigments between *ancestor d (P360)* and *frog (P425)* reveal that amino acid sites in TM IV–VII are also involved in the spectral tuning in *frog (P425)* (17). For unknown reason, the overall effect of amino acid changes in TM IV–VII on the λ_{max}-shift is negligible, whereas the λ_{max}-shift from *ancestor d (P360)* to *frog (P425)* can be explained by seven amino acid substitutions in TM I–III (17).

In the near future, other critical amino acid changes will be discovered and a more complete picture of amino acid interactions will emerge. When these additional critical amino acid changes in TM I–VII are found, the QM/MM method will need to be applied to these critical amino acid changes as well, which will allow fine tuning of the SWS1 pigments′ H-bond network. However, the results presented here are from various sets of amino acid changes and λ_{max}s of SWS1 pigments, and thus have a broad application and general implications for understanding the chemical mechanisms of UV and violet vision.

METHODS

Ancestral pigments

The amino acid sequences of ancestral pigments used in our QM/MM calculations have been inferred previously by applying PAML (23) to various ultraviolet and violet pigments in a wide range of vertebrates (4, 19). Specifically, *pigment a*, *pigment d*, *pigment f*, and *pigment h* in our analyses correspond to *pigment a*, *pigment b*, *pigment f*, and *pigment g*, respectively, in Shi and Yokoyama (4), while *pigment b* has been inferred in Tada et al (19) (Supplementary Figure 3).

Modeling the Structures and QM/MM calculations

The initial coordinates of the amino acids, 11-*cis*-retinal, and water molecules of each pigment were obtained by applying homology modeling (Modeler 9v7, www.salilab.org/modeller) to bovine rhodopsin (pdb code: 1U19). We followed standard protonation states for all amino acids except the following: 1) histidines, all of which are at the surface, are singly protonated, 2) Glu181 was taken neutral based on our PROPKA pKa calculations (see the discussions in ref. 8 and refs. therein). Relative stabilities and λs of SBR and PSBR analogs appear irrespective of Glu181 protonation state, 3) disulfide bond between Cys110 and Cys187, 4) acetylated methionine is used at the N terminus.

After protonating the modeled structures, the geometries were fully optimized at pure AMBER96 force field level (http://ambermd.org). They were further reoptimized by hybrid QM/MM calculations in the ONIOM electronic embedding scheme (QM = B3LYP/6–31G*; MM = AMBER) (9, 24). The QM portion includes 11-*cis*-retinal, Schiff base NH moiety, and Glu113 along with hydrogen link atoms. The general ONIOM methodology and the protocols adopted in this study have been described extensively elsewhere (8, 9, 19). In the following, we address the aspects relevant only to the present study.

We first modeled the ancestral pigments with PSBR (Supplementary Figure 4, panel a). We then gradually moved the hydrogen attached to the SB nitrogen toward one of the carboxylic oxygens of Glu113 (or Asp113 for the frog pigment) and performed QM/MM geometry optimization at each step by fixing only d_1. When the hydrogen atom was transferred to Glu113 (or Asp113), we fully optimized the structure at the QM/MM level to obtain the pigment with SBR (forward scan) (Supplementary Figure 4, panel b). We also performed an analogous energy scan on the resulting SBR analog of each pigment backward and obtain exactly the same initial PSBR analog. Therefore, PSBR and SBR analogs of the pigments given in this study are connected to each other via continuous energy paths. We introduced mutations on the QM/MM-optimized structures of the PSBR analogs of the ancestral pigments and performed extensive conformational searches for the mutated amino acids and their neighboring water molecules. The results given belong to the lowest energy conformers. Back mutations on the mutant pigments give exactly the same structure for the initial ancestral pigments. Therefore, the structural changes introduced by the mutations are reversible.

The individual contributions to δE were estimated by setting the charges of each atom in amino acids or waters to zero. Not only the charges of mutated and their neighboring amino acids or waters but also those near retinal and Glu113 moiety were set to zero to reveal the extent of their contributions to QM/MM energy difference. After finding the contributing amino acids or waters, we measured the geometry parameters involved with those fragments to reveal which structural changes are responsible for the δE energy separation. These analyses reveal that only three H-bond lengths (d_1, d_2 and d_3; Figure 2, panel d), which are already connected via a H-bond network, shows notable differences between ancestral and their mutant pigments, as given in Supplementary Table 1. When the charges of the amino acids at sites 114 and 118 are set to zero, the majority of the contribution to δE comes from the QM portion. This led us to compare the geometry parameters of the QM portion in both PSBR and SBR analogs of the ancestral and corresponding mutated pigments. The most significant change in the QM portion with mutations at sites 114 or 118 is the H-bond distance between SB nitrogen and Glu113/Asp113, i.e., d_1. This means that sites 114 or 118 regulate the chromophore-counterion distance d_1. The linear combination of the inverse of $d_1 - d_3$ distances, i.e., electrostatic energies, correlates well with ΔE. Although only the changes in the H-bond distances of $d_1 - d_3$ cause functional changes in the presently available pigment and mutant sets, it is possible that other H-bond distances of the given network may be modified by some other mutations and may also contribute to functional

changes. Although site 295 does not contribute to Δ*E*, it is important for the stabilization of W2 through an H-bond. In the presence of the pigments treated as AMBER charges, the vertical absorption wavelength (λ) of the retinal was evaluated at the QM = TD-B3LYP/6-31G* level (9, 22), leading to TD-B3LYP/AMBER level.

Supplementary Material

Refer to Web version on PubMed Central for supplementary material.

Acknowledgments

This work was supported by National Institutes of Health, Emory University, and Japan Science and Technology Agency.

References

1. Kito Y, Suzuki T, Azuma M, Sekoguti Y. Absorption spectrum of rhodopsin denatured with acid. Nature. 1968; 218:955–957. [PubMed: 5681237]
2. Ball S, Collins FD, et al. Studies in vitamin A; reactions of retinene1 with amino compounds. Biochem J. 1949; 45:304–307. [PubMed: 15392856]
3. Yokoyama S. Evolution of dim-light and color visual pigments. Annu Rev Genom Human Genet. 2008; 9:259–282.
4. Shi Y, Yokoyama S. Molecular analysis of the evolutionary significance of ultraviolet vision in vertebrates. Proc Natl Acad Sci USA. 2003; 100:8308–8313. [PubMed: 12824471]
5. Kusnetzow A, Dukkipati A, Babu KR, Singh D, Vought BW, Knox BE, Birge RR. The photobleaching sequence of a short-wavelength visual pigment. Biochemistry. 2001; 40:7832–7844. [PubMed: 11425310]
6. Dukkipati A, Kusnetzow A, Babu KR, Ramos L, Singh D, Knox BE, Birge RR. Phototransduction by vertebrate ultraviolet visual pigments: protonation of the retinylidene Schiff base following photobleaching. Biochemistry. 2002; 41:9842–9851. [PubMed: 12146950]
7. Fasick JI, Applebury ML, Oprian DD. Spectral tuning in the mammalian short-wavelength sensitive cone pigments. Biochemistry. 2002; 41:6860–6865. [PubMed: 12022891]
8. Altun A, Yokoyama S, Morokuma K. Color tuning in short wavelength-sensitive human and mouse visual pigments: Ab initio Quantum Mechanics/Molecular Mechanics studies. J Phys Chem A. 2009:11685–11692. [PubMed: 19630373]
9. Altun A, Yokoyama S, Morokuma K. Spectral tuning in visual pigments: an ONIOM(QM:MM) study on bovine rhodopsin and its mutants. J Phys Chem B. 2008; 112:6814–6827. [PubMed: 18473437]
10. Fujimoto K, JYH, Hayashi S, Nakatsuji H. On the color-tuning mechanism of Human-Blue visual pigment: SAC-CI and QM/MM study. Chem Phys Lett. 2006; 432:252–256.
11. Amora TL, Ramos LS, Galan JF, Birge RR. Spectral tuning of deep red cone pigments. Biochemistry. 2008; 47:4614–4620. [PubMed: 18370404]
12. Ramos LS, Chen MH, Knox BE, Birge RR. Regulation of photoactivation in vertebrate short wavelength visual pigments: protonation of the retinylidene Schiff base and a counterion switch. Biochemistry. 2007; 46:5330–5340. [PubMed: 17439245]
13. Hillebrecht JR, Galan J, Rangarajan R, Ramos L, McCleary K, Ward DE, Stuart JA, Birge RR. Structure, function, and wavelength selection in blue-absorbing proteorhodopsin. Biochemistry. 2006; 45:1579–1590. [PubMed: 16460005]
14. Sekharan S, Altun A, Morokuma K. Photochemistry of visual pigment in a G(q) protein-coupled receptor (GPCR) – Insights from structural and spectral tuning studies on squid rhodopsin. Chem Eur J. 2010; 16:1744–1749.
15. Sekharan S, Altun A, Morokuma K. QM/MM study of dehydro and dihydro beta-ionone retinal analogues in squid and bovine rhodopsins: Implications for vision in salamander rhodopsin. J Am Chem Soc. 2010; 132:15856–15859. [PubMed: 20964383]

16. Shi Y, Radlwimmer FB, Yokoyama S. Molecular genetics and the evolution of ultraviolet vision in vertebrates. Proc Natl Acad Sci USA. 2001; 98:11731–11736. [PubMed: 11573008]
17. Takahashi Y, Yokoyama S. Genetic basis of spectral tuning in the violet-sensitive visual pigment of African clawed frog, Xenopus laevis. Genetics. 2005; 171:1153–1160. [PubMed: 16079229]
18. Yokoyama S, Yang H, Starmer WT. Molecular basis of spectral tuning in the red- and green-sensitive (M/LWS) pigments in vertebrates. Genetics. 2008; 179:2037–2043. [PubMed: 18660543]
19. Tada T, Altun A, Yokoyama S. Evolutionary replacement of UV vision by violet vision in fish. Proc Natl Acad Sci USA. 2009; 106:17457–17462. [PubMed: 19805066]
20. Yokoyama S, Takenaka N, Agnew DW, Shoshani J. Elephants and human color-blind deuteranopes have identical sets of visual pigments. Genetics. 2005; 170:335–344. [PubMed: 15781694]
21. Yokoyama S, Takenaka N, Blow N. A novel spectral tuning in the short wavelength-sensitive (SWS1 and SWS2) pigments of bluefin killifish (Lucania goodei). Gene. 2007; 396:196–202. [PubMed: 17498892]
22. Wanko M, Hoffmann M, Strodel P, Koslowski A, Thiel W, Neese F, Frauenheim T, Elstner M. Calculating absorption shifts for retinal proteins: computational challenges. J Phys Chem B. 2005; 109:3606–3615. [PubMed: 16851399]
23. Yang Z. PAML 4: Phylogenetic analysis by maximum likelihood. Mol Biol Evol. 2007; 24:1586–1591. [PubMed: 17483113]
24. Vreven T, Byun KS, Komáromi I, Dapprich S, Montgomery JA Jr, Morokuma K, Frisch MJ. Combining quantum mechanics methods with molecular mechanics methods in ONIOM. J Chem Theory Comput. 2006; 2:815–826.

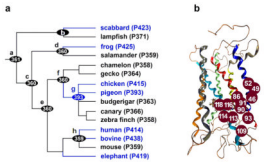

Figure 1.

Evolutionary characteristics of SWS1 pigments. (a) An evolutionary tree of SWS1 pigments. Species considered are scabbardfish (*Lepidopus fitchi*), lampfish (*Stenobrachius leucopsarus*), frog (*Xenopus laevis*), salamander (*Ambystoma tigrinum*), chameleon (*Anolis carolinensis*), gecko (*Gekko gekko*), chicken (*Gallus gallus*), pigeon (*Columba livia*), budgerigar (*Melopsittacus undulatus*), canary (*Serinus canaria*), zebra finch (*Taeniopygia guttata*), human (*Homo sapiens*), bovine (*Bos taurus*), mouse (*Mus musculus*), and elephant (*Loxodonta africana*). The numbers after P refer to experimental values. (b) The 12 currently known critical amino acid sites in TM I–III of SWS1 λ_{max} pigments (21). The structure and amino acid site numbers are taken from bovine rhodopsin (pdb code: 1U19).

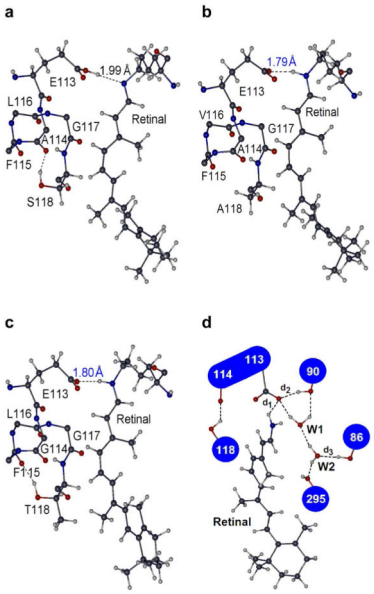

Figure 2.

The H-bond network of SWS1 pigments around site 114 that significantly affect the distance (d_1) between SB nitrogen and its Glu113 counterion (a) in *pigment a*. (b) in *pigment f'* (*pigment f* with F49V/F86S/L116V/S118A). (c) in *pigment h* with F46T/F49L/T52F/F86L/T93P/A114G/S118T. Only the energetically more stable pigment analog (SBR or PSBR) is shown. The numbers around SB nitrogen and carboxylic oxygen of Glu113 are the H-bond length (in Å) between them (black in SBR and blue PSBR analogs). (d) Schematic representation of the functionally important H-bond network of SWS1 pigments around 11-*cis*-retinal. Only polar groups of the amino acids are shown. H-bonds shown with broken lines are not present in all pigments and depend on the type of amino acids involved.

Table 1

Relative energies (ΔE) and calculated absorption wavelengths (λ) of SWS1 pigments and the corresponding experimental λ_{max} and $\Delta\lambda_{max}$

	h-7m[c]	**−3.1**	**480**	**63**	**411**	**50**
		QM/MM			**Experiment**	
pigment	**Mutation**	**ΔE(kcal·mol^{-1})**[a]	**λ (nm)**	**$\Delta\lambda$ (nm)**[b]	**λ_{max}(nm)**	**$\Delta\lambda_{max}$(nm)**[b]
a	-	6.2	417	0	361	0
d	-	5.6	410	−7	360	−1
	d-7m[c]	−5.6	475	58	421	60
f	-	3.8	422	5	360	−1
f′	-	−0.3	443[d]	26	393	32
	S86C	2.5	425	8	366	5
	S90C	3.6	413	−4	360	−1
	S86C/S90C	3.1	422	5	360	−1
h	-	8.3	425	8	359	−2
	F86S/L116V	−2.5	480	63	419	58
	F86Y	−2.4	482	65	424[e]	63

[a] was evaluated by subtracting the ground-state energy of a pigment with SBR from that ΔE of a pigment with PSBR. Positive (or negative) values indicate that pigments with SBR (or PSBR) are more stable than those with PSBR (or SBR).

[b] The $\Delta\lambda$ and $\Delta\lambda_{max}$ of a pigment are its $\lambda$and λ_{max} relative to those of *pigment a*.

[c] d-7m and h-7m correspond to *pigment d* with F86M/V91I/T93P/V109A/E113D/L116V/S118T (4) and *pigment h* with F46T/F49L/T52F/F86L/T93P/A114G/S118T (17), respectively.

[d] The λ of *pigment f′* is calculated by averaging the values of the pigments with PSBR (λ = 469 nm) and SBR (λ = 417 nm).

[e] Experiment was performed on mouse UV pigment rather than pigment h, both having λ_{max} of 359 nm.

Table 2

The change in ΔE of a mutant pigment relative to its ancestral pigment (δE) and individual contributions $\delta E_{113+114+118}$ (d_1), δE_{90+W1} (d_2), and δE_{86+W2} (d_3) in kcal·mol^{-1}

Pigment	Mutation	δE	$\delta E_{113+114+118}(d_1)$	$\delta E_{90+W1}(d_2)$	$\delta E_{86+W1}(d_3)$
a	Phe86 deletion	−0.4	4.4	−15.8	10.6
b	Phe86 deletion	−9.4	0.6	−18.3	9.1
b-*a*[a]	Phe86 deletion	−9.0	−3.8	−2.5	−1.5
d	d-7m	−11.2	−11.3	0.4	0.8
f	*f*′	−4.1	−4.2	0.9	−1.5
	f′/S86C	−1.3	−3.9	1.2	0.5
	f′/S90C	−0.4	−4.8	5.8	−2.4
	f′/S86C/S90C	−0.7	−4.1	6.3	−3.3
f′	S86C	2.8	0.3	0.3	2.0
	S90C	3.9	−0.6	4.9	−0.9
	S86C/S90C	3.4	0.1	5.4	−1.8
h	F86S/L116V	−10.8	−12.8	2.3	−3.1
	F86Y	−10.7	−12.8	2.3	−3.1
	h-7m	−11.4	−11.7	2.5	−3.2

[a]The difference in the first two rows.